

---

# SINGLE-CELL DATA ANALYSIS USING MMD VARIATIONAL AUTOENCODER

---

A PREPRINT

**Chao Zhang\***

Department of Computer Science  
Vrije Universiteit Amsterdam  
Amsterdam, 1081 HV  
c.zhang@vu.nl

April 18, 2019

## ABSTRACT

Variational Autoencoder (VAE) is a generative model from the computer vision community; it learns a latent representation of the images and generates new images in an unsupervised way. Recently, Vanilla VAE has been applied to analyse single-cell datasets, in the hope of harnessing the representation power of latent space to evade the “curse of dimensionality” of the original dataset. However, some research points out that Vanilla VAE is suffering from the issue of the less informative latent space, which raises a question concerning the reliability of Vanilla VAE latent space in representing the high-dimensional single-cell datasets. Therefore a study is set up to examine this issue from the perspective of bioinformatics.

This paper confirms the issue of Vanilla VAE by comparing it to MMD-VAE, a variant of VAE which has overcome this issue, across a series of mass cytometry and single-cell RNAseq datasets. The result shows MMD-VAE is superior to Vanilla VAE in retaining the information not only in the latent space but also the reconstruction space, which suggests that MMD-VAE be a better option for single-cell data analysis.

**Keywords** variational autoencoder · single-cell RNA seq · mass cytometry · deep learning · artificial intelligence · bioinformatics

## 1 Introduction

In recent years, deep learning has achieved much success in computer vision, speech recognition, natural language processing, audio recognition and so on. With this influence, deep learning has begun to percolate into many computational areas in computer science like probabilistic graphical models. Variational autoencoder (VAE)[1] is such a product of deep learning and probabilistic graphical models. Variational autoencoder has a deep neuron structure similar to autoencoder (see Figure 3) on the one hand and is a probability model in terms of original space (data  $x$ ) and latent space (latent variables  $z$ ) on the other hand[2].

For example, VAE can learn a latent space  $Z$  from the existing images  $X$  and generate new images  $x'$  that make sense to humans by sampling the latent space  $Z$ .

In recent years, the rapid development of biology experiment techniques like flow cytometry[3] and single-cell RNAseq[4] has led to a massive amount of high-throughput molecular data on a single cell level. Manual gating has been extensively used to determine new cell types from cytometry dataset, but the high dimensions make this operation less practical, especially when to discover new rare cell types[5]. Single-cell RNAseq has been able to capture the RNA expressions on a single cell level, which provides new possibilities in understanding the biological activities. Currently, the analysis of single-cell RNAseq data still revolves around the classifying and subsetting cell population in

---

\*<https://hi-it.org>

order to depict the cell heterogeneity[6] or constitution[7]. The analysis of multiple-cell high-dimensional datasets has challenged the capacity of the classical unsupervised learning methods, and therefore requires the development of new computational methods to deal with the complexity.

As an unsupervised learning method, the usage of VAE can be viewed from another perspective; that is, VAE learns a latent space  $Z$  that can represent the original space  $X$ . Especially, if  $x$  is high-dimensional and  $z$  is a low-dimensional, VAE seems to do something like dimension reduction and feature extraction, the traditional unsupervised learning strategy. This potential of VAE concurs with the interests of the bioinformatics community in reducing the dimensions of the multi-sample high-dimensional datasets for analysis. As a consequence, there have been a few explorative attempts[8][9][10][11] at applying VAE to single-cell datasets, hoping to harness of the representation power of the latent space to evade the “curve of dimension” of high-throughput data. All of the research above used VAE as a dimension reduction method in this regard.

Vanilla VAE is usually considered as the first choice when applying it to other domains like bioinformatics because it has been studied more thoroughly than its variants. However, previous computer vision research in VAE method has suggested that Vanilla VAE suffers from the issue of less informative latent features[12][13][14], which means the latent space might not be so meaningfully representative of the original space, potentially undermining the reliability of using VAE as a dimension reduction method. Meanwhile, MMD-VAE, using Maximum Mean Discrepancy (MMD) instead of Kullback–Leibler divergence as part of the training target, has overcome this issue[12], looking promising as an alternative to Vanilla VAE in bioinformatics and computational biology research.

In this paper, I have carried out an experimental study to examine the issue of the less informative latent space issue based on biological datasets as opposed to image datasets, hoping to bridge the gap between the instinct on the image datasets and that on the biological datasets. Briefly, the study compares Vanilla VAE and MMD-VAE based on the performance on the single-cell datasets of mass cytometry and RNAseq, confirms the issue on Vanilla VAE and further demonstrates the superior representativeness of latent space of MMD-VAE over Vanilla VAE.

## Results

### Classifier performance

The neural network classifier was applied to the four original datasets, AML, PAN and RBN have achieved a very high accuracy (Supplementary Table S1), while SN has achieved a moderate accuracy, which could be due to the different unsupervised methods used by the experts in the original papers to classify the datasets; the moderate accuracy here may reflect the disagreement between the classifier and the unsupervised method.

With regards to the classifier accuracy over the latent space of VAE, MMD-VAE outperforms Vanilla VAE across all the single-cell datasets, as Table 1 shows; incidentally, with regards to the classifier accuracy over the reconstruction space of VAE, MMD-VAE still outperforms Vanilla VAE across all the single-cell datasets (Table 2).

Dataset	Metrics	vanilla VAE	MMD-VAE
AML	F2	0.869+/-0.026	0.896+/-0.021
	MCC	0.891+/-0.030	0.917+/-0.009
PAN	F2	0.846+/-0.033	0.925+/-0.005
	MCC	0.870+/-0.029	0.933+/-0.005
SN	F2	0.364+/-0.064	0.576+/-0.041
	MCC	0.415+/-0.045	0.658+/-0.027
RBN	F2	0.901+/-0.032	0.964+/-0.007
	MCC	0.924+/-0.020	0.968+/-0.006

Table 1: The accuracy of neural network classifier over the latent space of VAE (the average accuracy+/-standard deviation).

### Performance of VAE

The running time of MMD-VAE is a little longer than Vanilla VAE (Figure 1), due to the relatively expensive calculation of MMD, if not the problem of code efficiency. In practice, across all the four datasets, the difference of the running time between two VAE architectures lies between 10 and 30 seconds. The reconstruction loss of MMD-VAE is generally smaller than that of Vanilla VAE in the experiment (Figure 2), which may correspond to the distinct classifier accuracies over the reconstruction space.

Dataset	Metrics	vanilla VAE	MMD-VAE
AML	F2	0.873+/-0.040	0.905+/-0.015
	MCC	0.893+/-0.035	0.922+/-0.008
PAN	F2	0.857+/-0.038	0.926+/-0.007
	MCC	0.875+/-0.032	0.933+/-0.006
SN	F2	0.454+/-0.050	0.752+/-0.024
	MCC	0.460+/-0.047	0.743+/-0.024
RBN	F2	0.928+/-0.027	0.974+/-0.003
	MCC	0.941+/-0.019	0.977+/-0.003

Table 2: The accuracy of neural network classifier over the reconstruction space of VAE (the average accuracy+/-standard deviation).

Besides, in the current experiment, MMD-VAE has less unlucky runs (1 unlucky run out of 23 runs across four datasets), those runs with worse performance (in terms of the accuracy of neural network classifier), than Vanilla VAE (6 unlucky runs out of 28 runs across four datasets). This observation may indicate that MMD-VAE is less subject to the stochastic property of architecture than Vanilla VAE; that is, MMD-VAE is more stable in getting a meaningful latent representation of the data.

## Discussion

Compared to the classifier accuracy achieved in the original datasets, in the reconstruction space and latent space of (Vanilla/MMD) VAE, the accuracy is lowered a little bit. This difference may be attributed to the nature of VAE architecture, which is pursuing an approximation, not exactness. This difference may also respond to the observation when VAE is applied to image data and that the newly generated image is still blurred. For those numbers in the biological datasets, the meaning usually does not come from the exactness of numbers, but the comparison between numbers; therefore the lowered accuracy may not hurt a thing.

In this study, one problem is to measure how much information can be retained in the latent space of VAE, which is most relevant to the bioinformatics research. Considering the widespread practice of the current biological research, I assume that the information equates the labels created by human experts (computational biologists) in the given datasets. Here I assume this information should be kept. Therefore it is reasonable to expect that the latent space and reconstruction space of VAE should be able to retain this information. To measure how much information is retained, I use a neural network classifier since it only works on the true data, not permuted data as the permutation test shows.

The comparison of two VAE architectures concerning how much information is retained is tricky because many subjective factors need to be considered. The parameters of VAE architectures and the neural network classifiers need to be optimized; the stochastic nature of neural networks and the complexity of datasets. In this study, I had held the expectation that MMD-VAE should be no worse than Vanilla VAE, so I optimized only the parameters of Vanilla VAE and its corresponding neural network classifier for each dataset, the result only reflects the efforts I had made to optimize, not the best possible result, which I couldn't guarantee to achieve. I reused these parameters for MMD-VAE and its corresponding neural network classifier accordingly; then I obtained the result. As long as the expectation that MMD-VAE outperforms Vanilla VAE holds, this experiment strategy should work; if not, this would only mean that MMD-VAE is no better than Vanilla VAE under this framework.

The result indicates the advantage of MMD-VAE over Vanilla VAE in retaining information of interest; MMD-VAE tends to run a little slower than Vanilla, due to the calculation of MMD. In practice, this may not be a big issue compared to the advantage of MMD-VAE over Vanilla VAE. For the reconstruction space, which is less of a focus in this paper, MMD-VAE also outperforms Vanilla VAE, well corresponding to the computer vision research where the generated image from MMD-VAE seems to be sharper than Vanilla VAE[15]. It may also correspond to the lower reconstruction loss of MMD-VAE (Figure 2). The reconstruction space seems to be worth further exploration, though the usage scenario is not explicit at first sight.

Admittedly, this research only covers the usage scenario that VAE is directly applied to datasets without further customization and change in its architecture (which would require extra explorations) in order to keep a comprehensive comparison still plausible, but I hope this comparison between MMD-VAE and Vanilla VAE can still give some intuition to people who intend to apply VAE to biological datasets in a more sophisticated way.

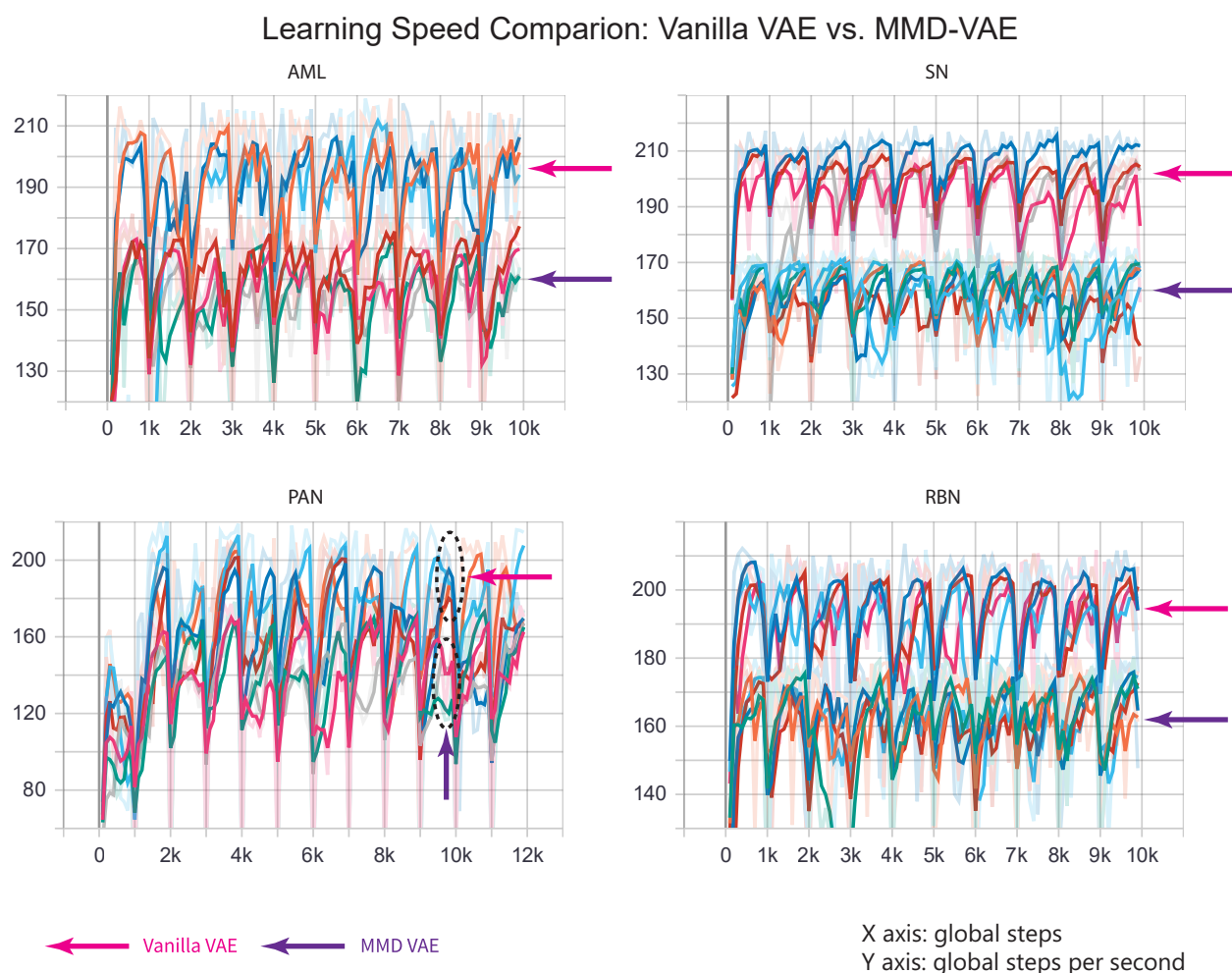


Figure 1: The training speed comparison between Vanilla VAE and MMD-VAE across four single-cell datasets. Each of the colourful lines represents a VAE run. The only difference between these two VAE architectures is the divergence, the calculation of MMD is more expensive, but thanks to the kernel embedding trick, the time it takes in practice is only a little longer than KL divergence. In the experiment, across all the four datasets, the difference of the running time between two VAE architectures lies between 10 and 30 seconds.

In summary, the issue of less informative latent space concerning Vanilla VAE probably limits the exploitation of its latent space to interpret the high-dimensional single-cell datasets; meanwhile, MMD-VAE does not have this issue. From these comparisons, I may draw the following conclusion: MMD-VAE could be a preferred option over Vanilla VAE when it comes to exploring the latent space for the biological data analysis.

## Methods

### VAE: a general overview

Variational Autoencoder (VAE) is a deep generative model with a flavour of both neural networks and probabilistic graphical models[2]. It learns the latent representation ( $z$ ) of the original space (data  $x$ ). At first glance, we could regard the VAE model as a simple graphical model (Supplementary Figure S1). In the inference period, the latent variables ( $z$ ) are sampled from a normal distribution, with fixed parameters ( $\theta$ ), new data  $X$  is generated; in the learning period,  $z$  and  $X$  are sampled  $N$  times and a neural network with a target (loss function) is trained to get the parameters  $\theta$ , that is, the parameters of the neural networks. When we use VAE as an unsupervised learning method, only the learning period fits the purpose, unless we want to generate new data. After the training (the learning period), we get the latent representation of dataset (original space).

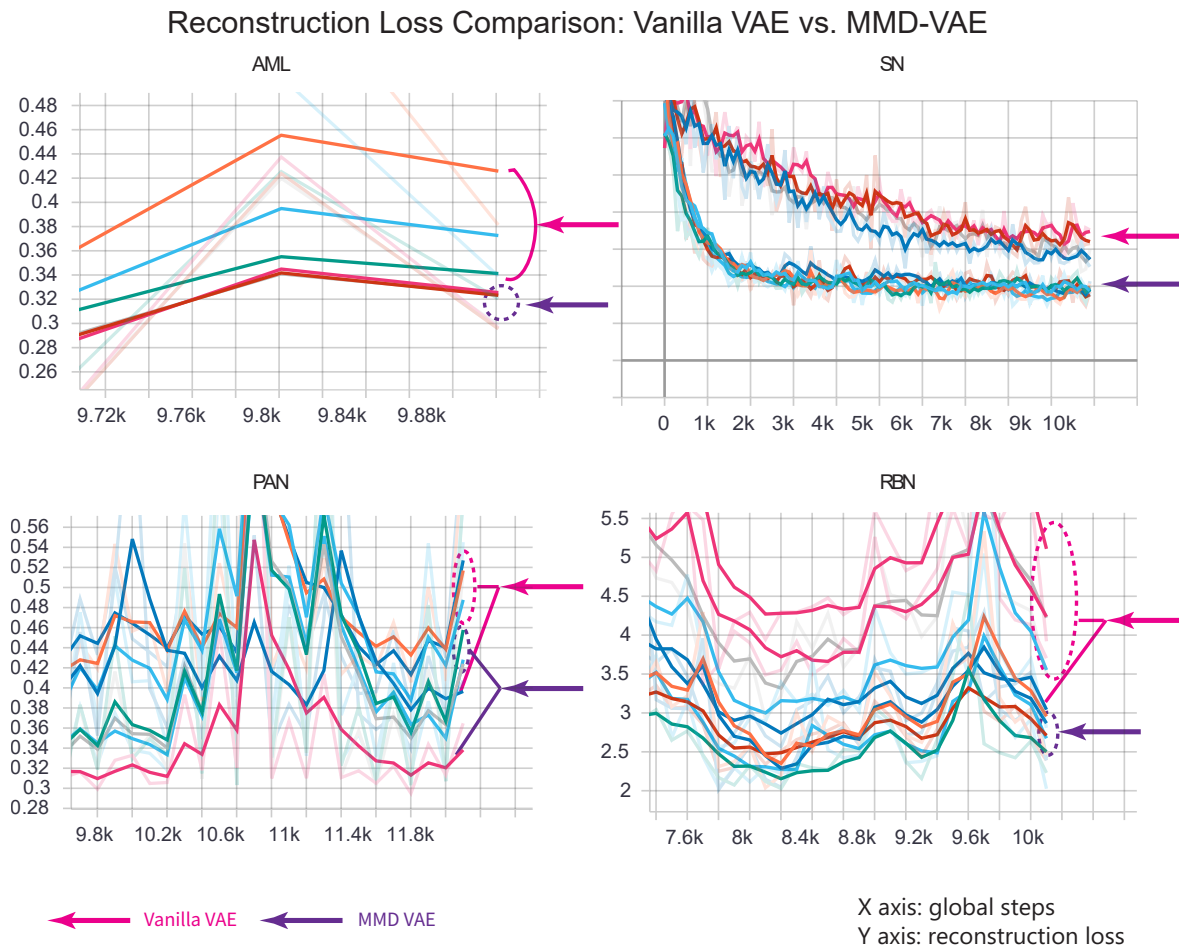
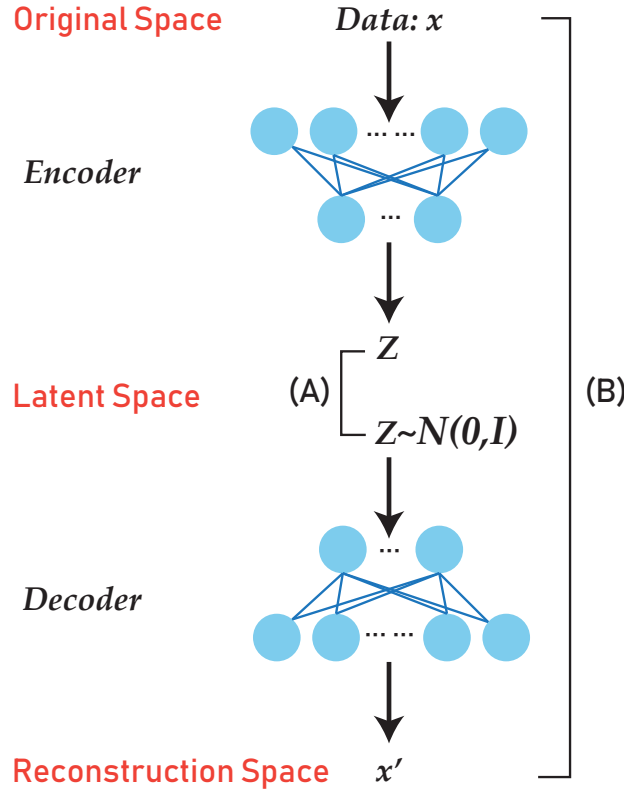


Figure 2: The reconstruction loss comparison between Vanilla VAE and MMD-VAE across four single-cell datasets. Each of the colourful lines represents a VAE run. MMD-VAE in general has a lower reconstruction loss than Vanilla, which may correspond to the distinct classifier accuracies over the reconstruction space.

To further understand how VAE works without being distracted by the technical details, we can view VAE in this way (Figure 3).  $P(X)$  is the distribution of the original space, that is, the dataset;  $q_\phi(z|x)$  is the encoding distribution, via which we get  $q_\phi(z)$ , the distribution of latent space; ideally, we sample  $z$  from a simple distribution  $p(z)$ , for example, a normal distribution, then via a decoding distribution  $p_\theta(x|z)$ , we get  $P(X')$  (we call it the reconstruction space hereafter).  $q_\phi(z|x)$  and  $p_\theta(x|z)$  are coded by neural networks ( $\phi$  and  $\theta$  are the parameters of the encoder and decoder). The training target includes two parts; the first part is “ $q_\phi(z)$  should be as similar as possible to  $p(z)$ , the simple distribution, say, a normal distribution”(A) in Figure 3); the second is “the original space  $P(X)$  and reconstruction space  $P(X')$  should be the same”(B) in Figure 3). The training target can be represented in equation (1), where  $D$  is any strict divergence, meaning that  $D(q||p) \geq 0$  and  $D(q||p) = 0$  if and only if  $q = p$ ,  $\lambda > 0$  is a scaling coefficient.

$$L = -\lambda D(q_\phi(z)||p(z)) + E_{p(x)} E_{q_\phi(z|x)} [\log p_\theta(x|z)] \quad (1)$$

In the Vanilla VAE model,  $D$  is Kullback–Leibler divergence, and  $\lambda = 1$  in the current study. so the first part of the formula 1 can be rewritten as  $E_{p(x)} [-KL(q_\phi(z|x)||p(z))]$



(A) and (B) are the training targets of variational autoencoder

Figure 3: An intuitive representation of variational autoencoder. (A) and (B) comprises the training target: (A),  $q_\phi(z)$  should be as similar as possible to  $p(z)$ , the simple distribution, say, a normal distribution; (B), the original space  $P(X)$  and reconstruction space  $P(X')$  should be the same.

### MMD-VAE

Maximum Mean Discrepancy (MMD) [16][17] is defined to measure the discrepancy between two distributions; it works based on the presumption that two distributions are identical if and only if all moments are identical[18].

In practice, a biased empirical estimate of the MMD is used by calculating empirical expectations computed on the samples  $X$  and  $Y$ , by equation (2), where  $F$  is a class of functions  $f : X \rightarrow \mathbb{R}$  and  $X$  is the space where  $x_i$  and  $y_i$  are defined.

$$MMD_b[F, X, Y] := \sup_{f \in F} \left( \frac{1}{m} \sum_{i=1}^m f(x_i) - \frac{1}{n} \sum_{i=1}^n f(y_i) \right) \quad (2)$$

When it comes to the implementation, MMD can be calculated efficiently via the kernel embedding trick[18], as equation (3)

$$MMD(p(z)||q(z)) = \mathbb{E}_{p(z), p(z')} [k(z, z')] + \mathbb{E}_{q(z), q(z')} [k(z, z')] - 2\mathbb{E}_{p(z), q(z')} [k(z, z')] \quad (3)$$

where  $k(z, z')$  is any universal kernel, such as Gaussian  $k(z, z') = e^{-\frac{\|z-z'\|^2}{2\sigma^2}}$ .

The difference of MMD-VAE from the stand VAE model is the divergence in the training target. In MMD-VAE, MMD is used instead of KL divergence.

Intuitively speaking, in terms of the implementation of MMD-VAE, for the two distributions  $p(z)$  and  $q(z)$ , as mentioned in equation (1) and (3),  $MMD(p(z), q(z))$  is a value calculated representing this discrepancy. The smaller  $MMD(p(z), q(z))$  is, the more similar  $p(z)$  and  $q(z)$  are.

All VAE architectures were implemented by TensorFlow [19] and TensorFlow Probability [20], visualised in TensorBoard, and run in Google Colaboratory (Colab) with GPU (Tesla K80) enabled.

## Datasets and data preprocessing

Single cell data usually mean mass cytometry (cyTOF) data and single-cell RNA-seq data. In this experiment, four published datasets were used; two are mass cytometry data; two, single-cell RNAseq data. These datasets are briefly summarized in Table 3. All of these datasets have been classified by the experts authoring the original papers using the computational methods described in these papers.

Dataset	Type	Cell No.	Class No.	Dimension	Supplement
AML	Mass Cytometry	104184	14	32	AML benchmark dataset
PAN	Mass Cytometry	102877	24	48	Panorama benchmark dataset
SN	scRNA-Seq	622	11	25334	Sensory Neurons, 55 principal components were used
RBN	scRNA-Seq	26830	18	13166	Retinal Bipolar Neurons, 37 principal components were used

Table 3: An overview of the datasets used in the study. Four datasets were used: two mass cytometry data and two single cell RNAseq data.

### Mass cytometry datasets

Dataset AML is a mass cytometry dataset of cryopreserved bone marrow aspirates from pediatric patients diagnosed with acute myeloid leukaemia. The data have been classified by the approach PhenoGraph from the original paper [21]. The data in use contain 104184 cells, 14 classes and have 32 dimensions.

Dataset PAN is a mass cytometry dataset from mice. The data have been classified (gated) by the algorithm “X-shift” from the original paper [22] already. The data in use contain 514386 cells, 24 classes and have 48 dimensions.

Both datasets have gone through the same preprocess where the data are rescaled by equation (4) where  $N_{original}$  is the original count of the dataset.

$$N_{new} = \log(1 + |N_{original}|) \quad (4)$$

### Single-cell RNAseq datasets

Dataset SN is the single-cell transcriptome dataset of mouse neurons classified in the original paper [7] by sampling, unsupervised grouping and comprehensive transcriptome analysis; the data in use contain 622 cells, 11 classes and have 55 dimensions (principal components extracted from 25334 dimensions (genes))

Dataset RBN is the single-cell transcriptome dataset of mouse retinal bipolar cells classified in the original paper [23] using unsupervised clustering; the data in use contain 26830 cells, 18 classes and have 37 dimensions (principal components extracted from 13166 dimensions (genes)).

Both single-cell RNAseq datasets have gone through Principal Component Analysis PCA (implemented in Python package: Scikit-learn[24]) first to reduce dimensions.

A permutation test [23] was reused to retain those principal components that capture statistically significantly correlated variation among the genes, which cannot be attributed to random “noise.” PCA was performed on  $N$  ( $N = 50$  in current experiment) randomized versions of the data, in each version of which, all the columns of the original expression data frame (genes) were randomly and independently permuted; then a threshold eigenvalue is calculated (the average of the maximum eigenvalues in each version of the randomized data); in the original data, any principal component whose eigenvalue is greater than the threshold is kept.

## Neural network classifier

To measure how much information has been retained in the latent space and reconstruction space of VAE, a neural network classifier is implemented in Keras to detect how many of the cells can still be correctly classified in the latent space and reconstruction space. Two metrics are used to measure the accuracy of the classifier: F2 score (F-measure in equation (5)) and Matthews correlation coefficient (equation (6)).

$$F_{\beta} = (1 + \beta^2) \cdot \frac{Precision \cdot Recall}{\beta^2 \cdot Precision + Recall} \quad (5)$$

where  $\beta = 2$  and  $Precision = \frac{TP}{TP+FP}$ ,  $Recall = \frac{TP}{TP+FN}$ .

$$MCC = \frac{TP \times TN - FP \times FN}{\sqrt{(TP + FP)(TP + FN)(TN + FP)(TN + FN)}} \quad (6)$$

TP = True Positive; FP = False Positive; FN = False Negative; TN = True Negative

A permutation test is also conducted to show that a neural network classifier only works over the original data, not the permuted data. For each permuted version of the dataset, the classification accuracy in terms of the two metrics mentioned above is on the random level. So the classifier can be confidently used.

The code is implemented by Keras 2.2.4[25] with Tensorflow[19] as the backend and run in Google Colab with GPU (Tesla K80) enabled.

## Experiment strategy

The parameter optimization can add much uncertainty to experiment to compare the two VAE architectures, therefore a proper strategy is needed to exercise the control over the uncertainty. In this study, VAE and neural network classifier go hand in hand in our mental model. Parameters has to be optimized dataset by dataset. For each dataset, parameters need to be trained only on the side of Vanilla VAE (including Vanilla VAE and its corresponding neural classifier); afterwards, the parameters are applied to MMD-VAE and its corresponding neural network classifier over the same dataset. The training was done manually. A complete list of the optimized parameters can be found in Supplementary Table S2 (VAE) and S3 (Classifier).

After the parameter optimization, Each VAE + neural network classifier is run five times over each dataset; due to the stochastic nature of VAE, it occasionally delivers bad results which can be detected intuitively by humans; this unlucky run is excluded from the final result.

The neural network classifier is trained on 22.5% of the dataset; 2.5% is used as the validation dataset; and 75% as the test dataset.

## Data availability

Data and code that contribute to the reproducibility of the results in this manuscript, as well as other technical details, are available at: <https://research-project.gitlab.io/mmd-vae>

## Acknowledgements

Thanks are given to Jaap Heringa and Sanne Abeln for the feedback on the manuscript. Thanks are given to Hui Liu for proofreading.

## Author contributions statement

C.Z. is the only author who contributes to every aspect of this work.

## Additional information

### Competing interests



The author declares no competing interests.

## References

- [1] Diederik P Kingma and Max Welling. Auto-Encoding variational bayes. December 2013.
- [2] Carl Doersch. Tutorial on variational autoencoders. June 2016.
- [3] Kieran O’Neill, Nima Aghaeepour, Josef Spidlen, and Ryan Brinkman. Flow cytometry bioinformatics. *PLoS Comput. Biol.*, 9(12):e1003365, December 2013.
- [4] Antoine-Emmanuel Saliba, Alexander J Westermann, Stanislaw A Gorski, and Jörg Vogel. Single-cell RNA-seq: advances and future challenges. *Nucleic Acids Res.*, 42(14):8845–8860, August 2014.
- [5] Lukas M Weber and Mark D Robinson. Comparison of clustering methods for high-dimensional single-cell flow and mass cytometry data: Comparison of High-Dim. cytometry clustering methods. *Cytometry*, 89(12):1084–1096, December 2016.
- [6] Efthymia Papalexi and Rahul Satija. Single-cell RNA sequencing to explore immune cell heterogeneity. *Nat. Rev. Immunol.*, 18(1):35–45, January 2018.
- [7] Dmitry Usoskin, Alessandro Furlan, Saiful Islam, Hind Abdo, Peter Lönnerberg, Daohua Lou, Jens Hjerling-Leffler, Jesper Haeggström, Olga Kharchenko, Peter V Kharchenko, Sten Linnarsson, and Patrik Ernfors. Unbiased classification of sensory neuron types by large-scale single-cell RNA sequencing. *Nat. Neurosci.*, 18(1):145–153, January 2015.
- [8] Z Wang and Y Wang. Exploring DNA methylation data of lung cancer samples with variational autoencoders. In *2018 IEEE International Conference on Bioinformatics and Biomedicine (BIBM)*, pages 1286–1289, December 2018.
- [9] Alexander J Titus, Carly A Bobak, and Brock C Christensen. A new dimension of breast cancer epigenetics - applications of variational autoencoders with DNA methylation. In *Proceedings of the 11th International Joint Conference on Biomedical Engineering Systems and Technologies*, pages 140–145. SCITEPRESS - Science and Technology Publications, 2018.
- [10] Dongfang Wang and Jin Gu. VASC: Dimension reduction and visualization of single-cell RNA-seq data by deep variational autoencoder. *Genomics Proteomics Bioinformatics*, 16(5):320–331, October 2018.
- [11] Gregory P Way and Casey S Greene. Extracting a biologically relevant latent space from cancer transcriptomes with variational autoencoders. In *Biocomputing 2018*, pages 80–91. WORLD SCIENTIFIC, February 2018.
- [12] Shengjia Zhao, Jiaming Song, and Stefano Ermon. InfoVAE: Information maximizing variational autoencoders. June 2017.
- [13] Xi Chen, Diederik P Kingma, Tim Salimans, Yan Duan, Prafulla Dhariwal, John Schulman, Ilya Sutskever, and Pieter Abbeel. Variational lossy autoencoder. November 2016.
- [14] Casper Kaae Sønderby, Tapani Raiko, Lars Maaløe, Søren Kaae Sønderby, and Ole Winther. Ladder variational autoencoders. February 2016.
- [15] Sigrid Keydana. TensorFlow for r: Representation learning with MMD-VAE. October 2018.
- [16] Arthur Gretton, Karsten M Borgwardt, Malte J Rasch, Bernhard Schölkopf, and Alexander Smola. A kernel Two-Sample test. *J. Mach. Learn. Res.*, 13(Mar):723–773, 2012.
- [17] Arthur Gretton, Karsten Borgwardt, Malte Rasch, Bernhard Schölkopf, and Alex J Smola. A kernel method for the Two-Sample-Problem. In B Schölkopf, J C Platt, and T Hoffman, editors, *Advances in Neural Information Processing Systems 19*, pages 513–520. MIT Press, 2007.
- [18] A tutorial on information maximizing variational autoencoders (InfoVAE). <https://ermongroup.github.io/blog/a-tutorial-on-mmd-variational-autoencoders/>. Accessed: 2019-3-22.
- [19] Martin Abadi, Ashish Agarwal, Paul Barham, Eugene Brevdo, Zhifeng Chen, Craig Citro, Greg S Corrado, Andy Davis, Jeffrey Dean, Matthieu Devin, and Others. Tensorflow: Large-scale machine learning on heterogeneous distributed systems. arxiv 2016. *arXiv preprint arXiv:1603.04467*, 2019.
- [20] Joshua V Dillon, Ian Langmore, Dustin Tran, Eugene Brevdo, Srinivas Vasudevan, Dave Moore, Brian Patton, Alex Alemi, Matt Hoffman, and Rif A Saurous. TensorFlow distributions. November 2017.

- [21] Jacob H Levine, Erin F Simonds, Sean C Bendall, Kara L Davis, El-Ad D Amir, Michelle D Tadmor, Oren Litvin, Harris G Fienberg, Astraea Jager, Eli R Zunder, Rachel Finck, Amanda L Gedman, Ina Radtke, James R Downing, Dana Pe'er, and Garry P Nolan. Data-Driven phenotypic dissection of AML reveals progenitor-like cells that correlate with prognosis. *Cell*, 162(1):184–197, July 2015.
- [22] Nikolay Samusik, Zinaida Good, Matthew H Spitzer, Kara L Davis, and Garry P Nolan. Automated mapping of phenotype space with single-cell data. *Nat. Methods*, 13(6):493–496, June 2016.
- [23] Karthik Shekhar, Sylvain W Lapan, Irene E Whitney, Nicholas M Tran, Evan Z Macosko, Monika Kowalczyk, Xian Adiconis, Joshua Z Levin, James Nemesh, Melissa Goldman, Steven A McCarroll, Constance L Cepko, Aviv Regev, and Joshua R Sanes. Comprehensive classification of retinal bipolar neurons by Single-Cell transcriptomics. *Cell*, 166(5):1308–1323.e30, August 2016.
- [24] F. Pedregosa, G. Varoquaux, A. Gramfort, V. Michel, B. Thirion, O. Grisel, M. Blondel, P. Prettenhofer, R. Weiss, V. Dubourg, J. Vanderplas, A. Passos, D. Cournapeau, M. Brucher, M. Perrot, and E. Duchesnay. Scikit-learn: Machine learning in Python, 2011.
- [25] François Chollet et al. Keras. <https://keras.io>, 2015.